J Nanostruct 15(2): 752-761, Spring 2025

RESEARCH PAPER

Synthesis of Faceted Thin Diamond Film on High Purity Nickel Substrate by PECVD Technique

Zahra Khalaj

Department of Physics, Shahr-e-Qods Branch, Islamic Azad University, Tehran, Iran

ARTICLE INFO

Article History:
Received 03 January 2025
Accepted 26 March 2025
Published 01 April 2025

Keywords:
Graphite
Nano-crystalline diamond
Magnetic Field (MF)
Plasma Enhanced Chemical Vapor Deposition (PECVD)

ABSTRACT

In the present study, Nano-crystalline Diamond (NDs) coatings were deposited on nickel substrates by a DC-plasma enhanced chemical vapor deposition (DC-PECVD) deposition technique using methane/hydrogen (CH_4/H_2) gas mixtures. Due to the extremely high surface energy of diamond, the nucleation and growth of diamond phase on non-diamond substrate is difficult. In order to improve the diamond nucleation density to form continuous films, a good pretreatment using suitable etching gas and magnetic field (MF) were used. The effects of MF pre-treatment on the characteristics of deposited coatings are discussed in view of experimental studies using analytical techniques such as Raman spectroscopy, X-ray diffraction pattern (XRD) and field-emission scanning electron microscopy (SEM). It was found that the quality of the diamond films grown with MF pre-treatment much higher than the film grown without MF pre-treatment process. The research indicates that the new technology of diamond growth using MF may have incredible effect on CVD diamond production at low temperature and few hours.

How to cite this article
Khalaj Z. Synthesis of Faceted Thin Diamond Film on High Purity Nickel Substrate by PECVD Technique. J Nanostruct, 2025; 15(2):752-761. DOI: 10.22052/JNS.2025.02.033

INTRODUCTION

Over the past few years, carbon-based materials such as diamond, carbon nanotubes (CNTs), diamond like carbon (DLC), fullerene and graphene have aroused intensive research interest from both scientific and engineering communities due to the unique superlative properties. Among these materials, diamond films, sp^3-bonded carbon have been considered as strategic nanomaterials for applications in a variety of current and future systems owing to their extraordinary properties including: high hardness, optical transparency, thermal conductivity, wear resistance, lowest compressibility, unique semiconductor characteristics, inertness towards most chemical and reagents intrinsically low friction [1]. These outstanding features of diamond motivated the exploitation of this carbon nanostructure in various applications ranging from wear resistant coatings, cutting tools for non-ferrous materials, as heat spreaders for electronic devices, flat panel displays and transparent windows for infrared light [1-5], and so on. Furthermore, compared to the microcrystalline diamond (MDs) thin film, Nano-crystalline Diamond (NDs) films with smaller grains have attracted great attention in different fields such as a promising cold cathode field emission material, beholden to its lower turn-on field, high power at high temperature, high stability and reliability on service and high current

* *Corresponding Author Email: z.khalaj@qodsiau.ac.ir*

density [6, 7]. This fact increases the power of NDs films for valuable applications in vacuum electronic devices like microwave amplifier and field emission displays [7]. However, it is noticeable that the practical use of diamond films in many scientific and industrial sectors is limited owing to its high-cost and scarcity [5]. Nowadays, numerous techniques have been developed for producing diamond films, including: pulsed laser deposition (PLD) [8], microwave plasma chemical vapor deposition [9], plasma enhanced chemical vapor deposition (PECVD) [10, 11], hot filament chemical vapor deposition (HFCVD) [12-15] and etc. Based on the unique structure of diamond with fully sp^3 bonded form of black carbon, it has some challenges to growth on CVD techniques. Among these methods, plasma enhanced chemical vapor deposition has been widely used in diamond synthesis, due to its large surface deposition, easy processing, low capital cost and film uniformity control over deposition parameters[16, 17]. All parameters are so sensitive and should be rather balanced to form a high crystalline quality of this structure. Diamond growth starts when carbon atoms on the surface begin to nucleate and form SP^3 bonds in the tetrahedral lattice.

There are two types of diamond growth which called Homogeneous and non-Homogeneous growth. In homogeneous type, a diamond base substrate or diamond seed is used. Then, the only thing that is necessary for the creation of a tetrahedral network is the diamond network which placed on the surface atom by atom in the vapor deposition process. In non-homogeneous type, a non-diamond substrate is used for growth, so the carbon atoms have no pattern on the substrate to follow and won't come together atom by atom like in the previous case. Therefore, after hitting the surface of the substrate, carbon atoms immediately cause surface etching and then return to the gas phase and react with hydrogen atoms. To avoid this problem, before the diamond growth process begins, the substrate must be pre-treated for the reaction. Using diamond base substrate or diamond seed is not commercial and also limits the type of substrate and applications. Therefore, using different type of substrate without diamond seed and improving the synthesis quality is one of the scientist's problems during recent years [1-7,9-17].

Furthermore, it is noticeable that due to the extremely high surface energy of diamond, the nucleation and growth of diamond phase on non-diamond materials is difficult [18, 19]. In order to improve the diamond nucleation density to form continuous films, a good pretreatment of the substrates is usually needed [18]. Over the years, different methods for surface pretreatment have been developed, including scratching, seeding, electrical biasing, laser processing, various types of chemical and physical etching and chemical treatments, to improve substrate surface qualification before diamond deposition [18]. But none of them is not absolutely ideal method for perfect quality of produced diamond.

In addition, it has been reported that the nucleation density and the grain growth rate of the diamond besides viscosity are also affected by the magnetic field [19-22]. In this study, a DC-PECVD system were used to obtain a uniform deposition with a low cost of production. In addition, to make a high-density diamond film without using diamond powder for seeding, an etching treatment were used on Ni substrate using H_2 plasma with combination of Magnetic field in pre-treatment step. This manuscript is organized as follows; following the introduction in Section 1 the experimental details are described in Section 2, Section 3 is dedicated to results and discussion and finally conclusion is presented in Section 4.

MATERIALS AND METHODS

Substrate Pre-Treatment

Nickel wafers (Ni) with 99.99% purity were used as the substrates in this experiment and pre-treated in two steps: All the substrates were polished with diamond paste (1µm) to obtain a smooth surface. Before loading into deposition chamber, the Ni substrates (5mm×5mm) were ultrasonically cleaned in bath of acetone, ethanol and de-ionized water for 15 minutes. The samples called #1 and #2 were kept in desiccators in vacuum. Sample #2 was kept in the vicinity of two magnets for 48h before loading the reaction chamber. The Magnetic Field (MF) applied in this pre-treatment process was 1.2T. A rectangle cubic magnet was used. The Magnetic field was parallel with surface.

CVD diamond growth

The experiment is performed on the DC-Plasma Enhanced chemical vapor deposition (PECVD) system. Fig. 1 shows the schematic diagram of the PECVD system.

The main central chamber of the system is a cylindrical box with a diameter of 28cm consisting of metallic base and a cover. The DC source is flanged on the top of the system cover. In order to insert the substrates inside the chamber, an Aluminum cover open from top. The door handling by vertical shifting the cover on top of the system. The chamber is pre-evacuated by rotary pump up to the base pressure of the 10^{-2} Torr. All substrates were placed on a furnace right under the anode. The temperature of the substrates is monitored by a sensitive thermocouple. In both experiments, for pre-treating the substrates, the etching process was used. An argon gas was inserted to the system for 5 minutes to clean the system and removing the oxide layers. The substrate temperature, flow rate, and etching pressure were: 550°C, 50 sccm, and 5 Torr, respectively. For creating the suitable sites for the first nucleation, the hydrogen gas was used about 20 minutes in 600°C with the flow rate of 20 sccm. The etching pressure in this case was 8 Torr. For growing process, a mixture of methane and hydrogen with~ 8% flow ratio were used for growing the NDs. The applied current and voltage in this experiment were 50 mA and 400 kV respectively.

RESULTS AND DISCUSSION

Raman Spectroscopy

Raman spectroscopy is a standard non-destructive nano-materials characterization technique that is widely used for the analysis of structural typicality of carbonaceous materials, such as Diamond [23], [24], [26-27], Diamond-like carbons (DLCs) [28,29], nanotubes (CNT) [30] and [31]. The Gaussian deconvoluted Raman spectra in the frequency range from of 1000-1800 cm^{-1} of the deposited films magnetic field is shown in Fig. 2. The fitted spectra exhibited many overlapped features. It is clearly observed that the obvious features at 1332 cm^{-1}, 1351 cm^{-1} and 1578 cm^{-1}, exist in the Raman spectra of deposited coatings which are attributed to diamond of sp^3-bonded carbon (T_{2g} mode) [32], D and G band of sp^2-bonded carbon [33], respectively. The vibrational band of D peak originated from the breathing modes of sp^2-bonded carbon atoms in aromatic rings. This mode represents disorder in sp^2 sites belonging to carbon framework [34, 35], while the G peak for carbon materials arises from the bond stretching of all pairs of sp^2 atoms present in both rings and chains [34].

In addition, the characteristic peak located at 1440 cm^{-1} as a major sign of NDs is belong to the vibration of C-H bonds in trans-polyacetylene (TPA) structure which provides indirect evidence that the hydrogen has been incorporated into the samples, specifically, at the grain boundaries [23, 36]. Furthermore, the presence of other feature at 1245 cm^{-1} in these spectra is also associated with

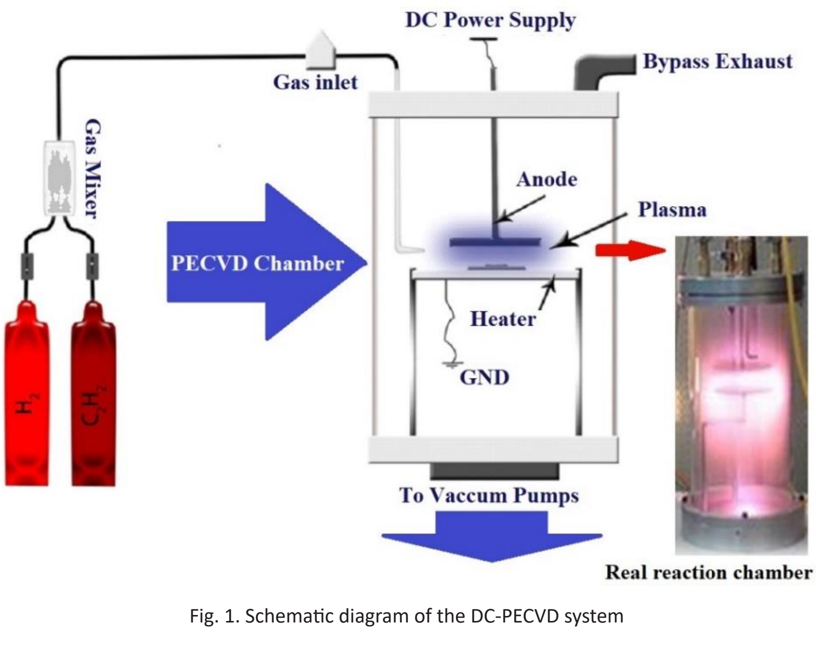

Fig. 1. Schematic diagram of the DC-PECVD system

NDs [37]. Moreover, the obvious characteristic peak locating at 1540 cm^{-1} characterizes the diamond-like carbon structure [38]. The peak at 1607 cm^{-1} is assigned to nanocrystalline graphite [39]. It is clear that Raman spectrum of the diamond film deposited with MF pre-treatment, as shown in Fig. 2b, has a sharp peak at 1332 cm^{-1}, which indicates. On the other hand, a weak peak at around 1332 cm^{-1} appears on the Raman spectrum of the diamond film deposited without MF (Fig. 2a), implying that poor quality. It is generally considered that the area intensity ratio of diamond peak to G peak (I_{Dia}/I_G) could be used to assess the relative amount of sp^3 phase [7]. Through multi-Gauss fitting, the I_{Dia}/I_G ratio of the diamond films deposited with the MF is found to be 8.7, while that of the diamond films deposited without MF is around 7.3. The former is higher than the latter, indicating that the quality of diamond film deposited with MF is much better than that deposited without MF pre-treatment.

Crystallinity Analysis

X-Ray diffraction (XRD) is one of the powerful techniques which contributes detailed information about the chemical composition and crystallographic structure of the materials [40-42]. The XRD patterns of deposited coatings at with and without MF pre-treatment are shown in Fig. 3. In the sample 3(a), we can see reflection peak at 2θ= 27.98° belongs to methane phase. Moreover, the other diffraction peaks at 2θ angles of 38.60° and 39.66° are detectable that are attributed (020) and (-102) methanol phase, respectively. In addition, several reflections at 2θ= 23.49°, 40.66°, 42.50°, 48.05°, 69.34° and 74.35° corresponding to the plans of (009), (0 0 24), (012), (1 0 13), (1 0 19) and (0 0 42) characteristic of graphite structure can be clearly observed. Furthermore, Rhombohedral diamond phase has two diffraction at 2θ= 41.46° and 46.40° corresponding to (101) and (107) originations, respectively, the other reflection peaks assigned to graphite 26.06° and Ni, 45.02° are also detected in this sample. According to results in 3(b), we can see that the XRD pattern of the deposited sample with MF pre-treatment dramatically changes. Diffraction peak with strongly sharp intensity at 2θ angle of 44.62° attributing to the (103) reflection plane of hexagonal diamond can be seen in this sample. Furthermore, the other reflection peaks at 2θ=51.62° and 93.11° belong to (0 1 17) and (200) graphite planes also is clearly observed. In addition, three diffraction peaks appear at 2θ =76.49°, 98.40° and 122.03° assigned to (220), (222) and (400) reflection planes of Ni, respectively. XRD spectra indicate that the phase transition occurs and the preferred orientation of the Rhombohedra diamond films transforms from (101) and (107) to (103) hexagonal diamond phases.

SEM Analysis

Fig. 4 shows typical SEM images of the films deposited MF at 600˚C in PECVD reactor. It can be seen in Fig. 4 that the morphology of the surface mostly covered by Graphite and amorphous

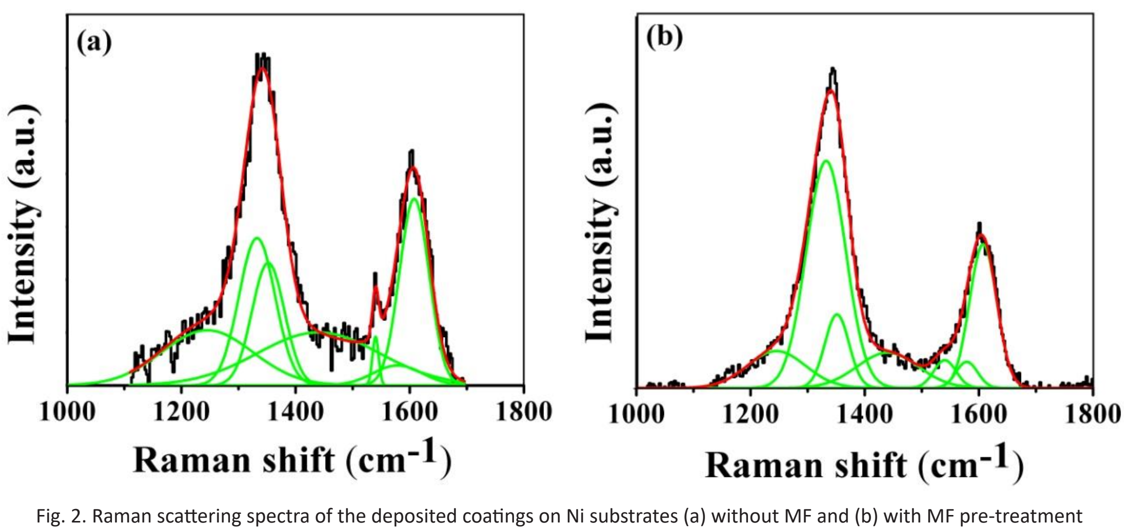

Fig. 2. Raman scattering spectra of the deposited coatings on Ni substrates (a) without MF and (b) with MF pre-treatment

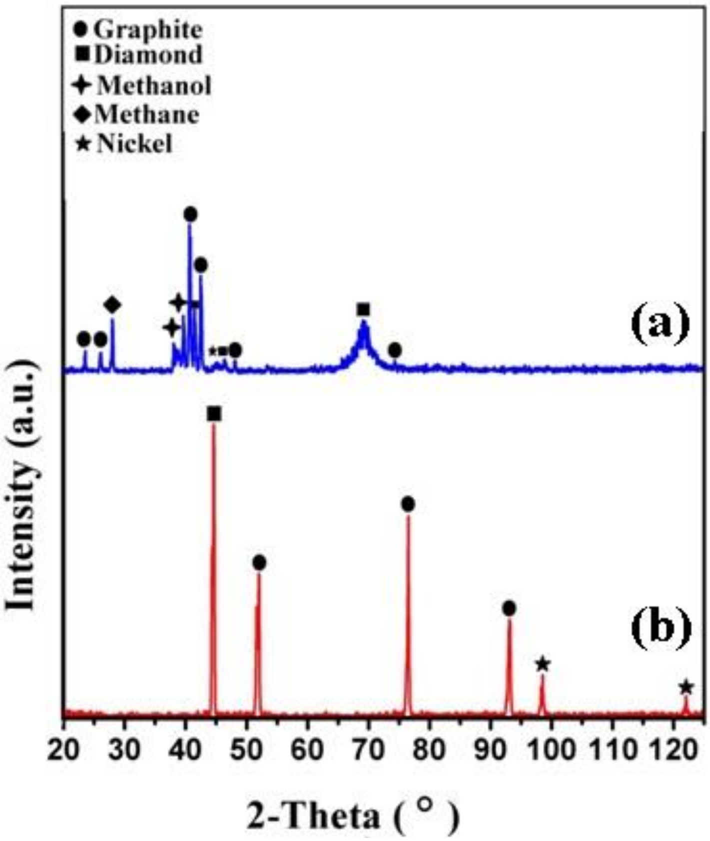

Fig. 3. X-ray diffraction patterns of the deposited coatings (a) MF and (b) with MF pre-treatment

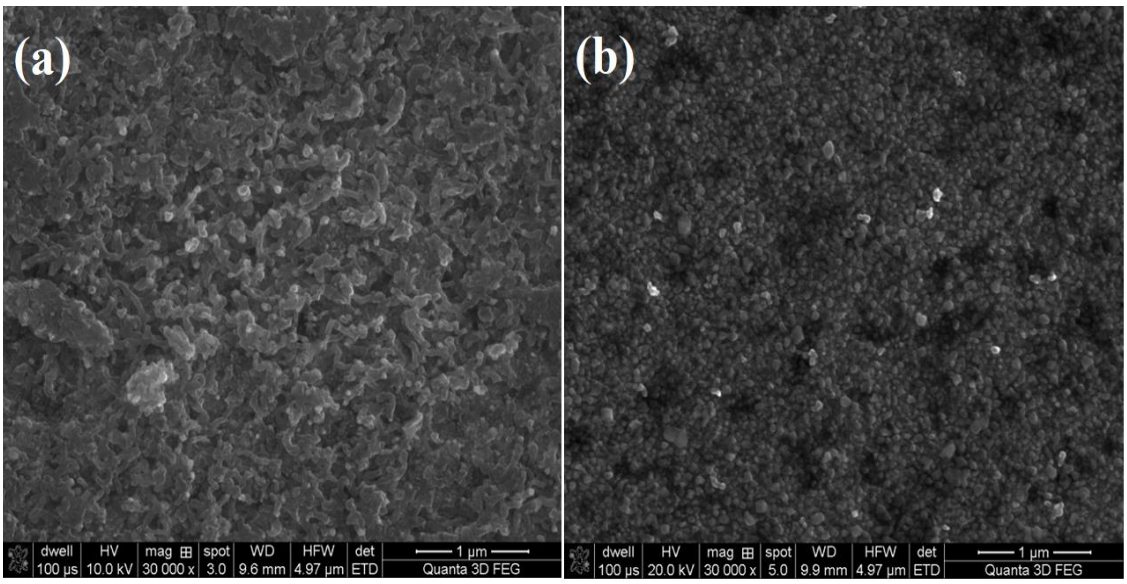

Fig. 4. Typical SEM images of deposited films on high purity Nickle substrate with PECVD system pre-treated (a) without MF (b) with MF

phase of carbon. However, high quality crystalline diamond was observed in sample #2.

The surface images were recorded using FEI Quanta 3D FEG 200/600 Scanning Electron Microscope Dual Beam: FEB and FIB. The morphology of the samples was studied here. In order to investigate the scenario of what happened in the sample #1, the cutting process was performed by using the ions beam (30 pA). After cutting with the ions beam, it was performing the scanning by using the electrons beam in order to obtain a better image. The elemental analyses was achieved with an EDAX Genesis device attached on the FEI scanning electron microscope. It can be observed that the sample #1 content preponderantly carbon according with the diamond phase identified in XRD pattern and a small amount of oxygen. For a more detailed morphological analysis there was performed a cross section using high-current ion column (Fig. 5). Quanta 3D FEG's high-current FIB enables fast material removal. Automated FIB sectioning recipes enable accurate cross-sectioning. Automated FIB sectioning recipes enable accurate cross-sectioning and low damage sample cleaning.

Table 1 shows the elemental analyze in cross section figure contain Ni 42.43% at. and Ga 6.50% at., in the area where it was made the cut using ion beam. Ni comes from the substrate on which diamond is deposited on and Ga can appear because the cross-section is made by using high-current ion column with Ga liquid-metal ion source.

In order to investigate the morphology of the surface in sample #1, the EDAX Genesis device attached on the FEI scanning electron microscope to observe content mostly carbon according and a small amount of oxygen (Fig. 6). The mentioned mark in SEM photo of Fig. 6 shows the EDAX result which described in detail in Table 2.

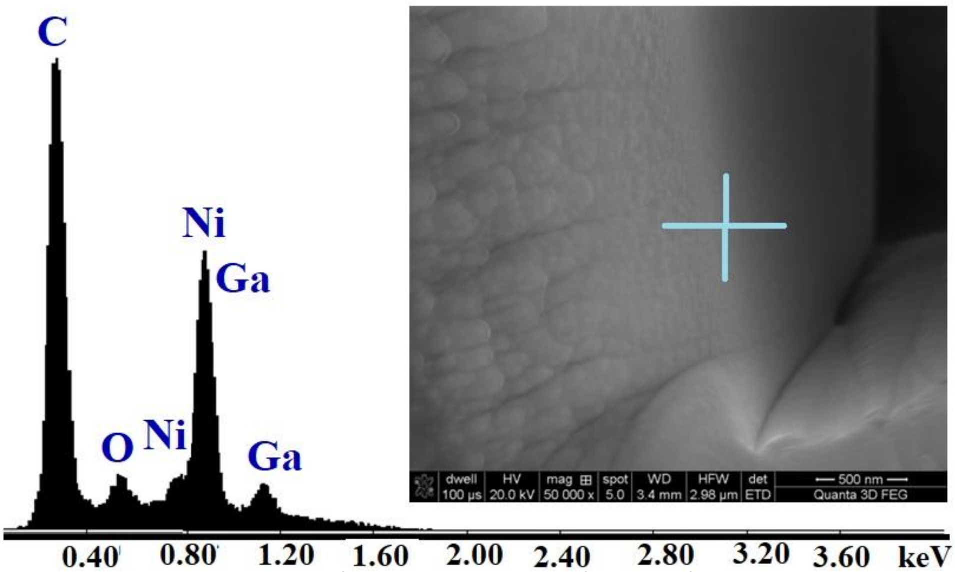

Fig. 5. The cross-section image of SEM and the EDAX result of sample #1 from marked point place.

Table 1. The result of the EDAX analysis from inside of the of sample #1 cutting with the ions beam

Element	Wt%	At%	K-Ratio	Z	A	F
C K	15.43	45.97	0.1950	1.4623	0.8640	1.0001
O K	2.28	5.10	0.0295	1.3597	0.9500	1.0007
Ni L	69.61	42.43	0.6357	0.9161	0.9967	1.0002
GaL	12.67	6.50	0.1000	0.8218	0.9599	1.000
Total	100.00	100.00				

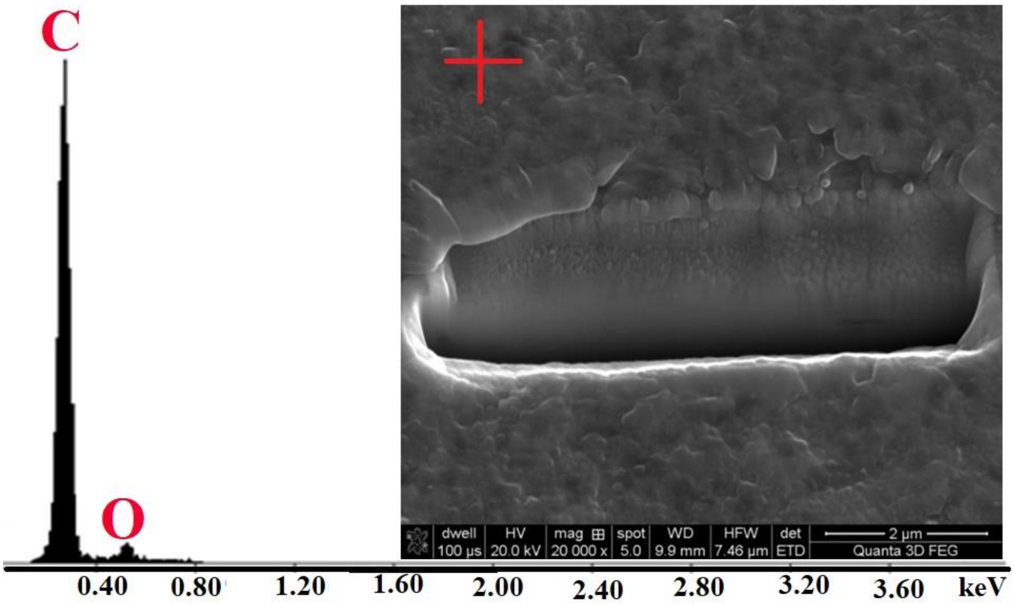

Fig. 6. The cross-section image of SEM and the EDAX result of the marked point place on the surface in sample #1.

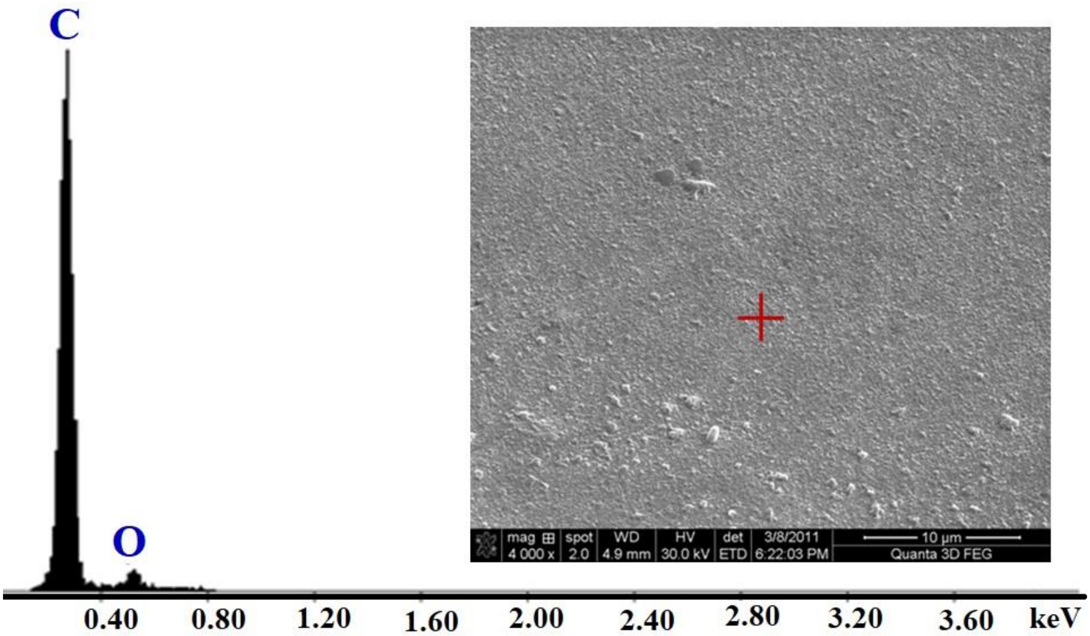

Fig. 7. The SEM image and the EDAX result of the marked point place on the surface in sample #2.

Table 2. The result of the EDAX analysis from the surface of the sample #1

Element	Wt%	At%	K-Ratio	Z	A	F
C K	0.00	90.41	0.8822	1.0082	0.9986	1.0000
O K	0.00	9.59	0.1146	0.9452	0.9802	1.0000
Total	100.00	100.00				

Table 3. The result of the EDAX analysis from the surface of the sample #2

Element	Wt%	At%	K-Ratio	Z	A	F
C K	0.00	92.44	0.9066	1.0065	0.9989	1.0000
O K	0.00	7.56	0.0909	0.9437	0.9797	1.0000
Total	100.00	100.00				

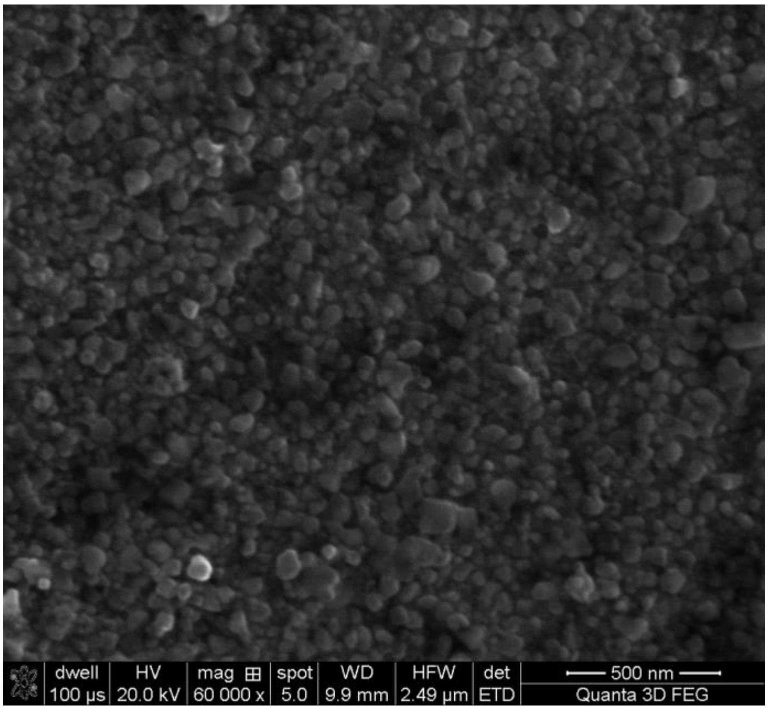

Fig. 8. High quality faceted thin diamond film synthesized on Ni substrate using MF and etching pre-treatment.

Fig. 7 shows the SEM image of diamond film covered the Ni substrate homogeneously which is completely due to the good pre-treatment with magnetic field that has a strong effect on producing faceted diamond on substrate. The EDAX were taken from the marked point (Table 3). The results show the highly amount of Carbon 92.44 at% and a few oxygens.

It can be seen in Fig. 8 that the average grain size of diamond deposited with MF pre-treatment is about 40 nm. The results indicated MF pre-treatment has a significant effect on grow thing high quality diamond film with (103) crystalline structure. Therefore, the results show that, for producing perfect quality of diamond and successfully coaching carbon atoms to find a suitable algorithm for growth in substrate, a combination of magnetic field before loading to the chamber and etching gas before main reaction is a perfect choice [40-50]. This combination was a novel method for diamond production. The obtained results show a high quality of diamond film production on substrate surface [43-52].

Fig. 8. High quality faceted thin diamond film synthesized on Ni substrate using MF and etching pre-treatment.

CONCLUSION

In the present work, nanocrystalline diamond have been deposited on Ni substrates by utilizing DC-PECVD deposition technique and the influence of MF pre-treatment on the structure and surface morphology of the deposited films was investigated. The experimental results show that the MF pre-treatment plays undeniable role on the characteristics of the deposited samples. It has been found that the diamond films deposited with MF pre-treatment condition have good crystallinity and high quality.

CONFLICT OF INTEREST

The authors declare that there is no conflict of interests regarding the publication of this manuscript.

REFERENCES

1. Gracio JJ, Fan QH, Madaleno JC. Diamond growth by chemical vapour deposition. J Phys D: Appl Phys. 2010;43(37):374017.
2. Rani R, Panda K, Kumar N, Sankaran KJ, Ganesan K, Lin IN. Tribological Properties of Ultrananocrystalline Diamond Films in Inert and Reactive Tribo-Atmospheres: XPS Depth-Resolved Chemical Analysis. The Journal of Physical Chemistry C. 2018;122(15):8602-8613.
3. Yates L, Sood A, Cheng Z, Bougher T, Malcolm K, Cho J, et al. Characterization of the Thermal Conductivity of CVD Diamond for GaN-on-Diamond Devices. 2016 IEEE Compound Semiconductor Integrated Circuit Symposium (CSICS); 2016/10: IEEE; 2016. p. 1-4.
4. Yeh C-J, Chang H-T, Leou K-C, Lin IN. Plasma post-treatment process for enhancing electron field emission properties of ultrananocrystalline diamond films. Diamond Relat Mater. 2016;63:197-204.
5. Ajikumar PK, Ganesan K, Kumar N, Ravindran TR, Kalavathi S, Kamruddin M. Role of microstructure and structural disorder on tribological properties of polycrystalline diamond films. Appl Surf Sci. 2019;469:10-17.
6. Pradhan D, Lin IN. Grain-Size-Dependent Diamond–Nondiamond Composite Films: Characterization and Field-Emission Properties. ACS Applied Materials & Interfaces. 2009;1(7):1444-1450.
7. Long H, Li S, Luo H, Wang Y, Wei QP, Yu ZM. The effect of periodic magnetic field on the fabrication and field emission properties of nanocrystalline diamond films. Appl Surf Sci. 2015;353:548-552.
8. Hara T, Yoshitake T, Fukugawa T, Zhu Ly, Itakura M, Kuwano N, et al. Nanocrystalline diamond film prepared by pulsed laser deposition in a hydrogen atmosphere. Diamond Relat Mater. 2004;13(4-8):679-683.
9. Hu W, Chen K, Tao T, Yu X, Zhou J, Xie Z, et al. High-rate growth of single-crystal diamond with an atomically flat surface by microwave plasma chemical vapor deposition. Thin Solid Films. 2022;763:139571.
10. Asgary S, Jafari A, Ebrahminejad Z, Ardaheh M. Evolution of physical properties of diamond nanoparticles deposited by DC-PECVD method after post deposition annealing. Journal of Materials Science: Materials in Electronics. 2019;30(23):20451-20458.
11. Xu Q, Yang GM. Nucleation and growth of nanocrystalline diamond on NaCl substrate by RF-PECVD. Journal of Physics and Chemistry of Solids. 2013;74(4):541-544.
12. Haddad M, Kurtulus O, Mertens M, Brühne K, Glüche P, Fecht H. Optimization of residual stresses inside diamond thin films grown by hot filament chemical vapor deposition (HFCVD). Diamond Relat Mater. 2023;131:109564.
13. Azari M, Iranmanesh A, Diudea MV. Vertex-Eccentricity Descriptors in Dendrimers. Studia Universitatis Babeş-Bolyai Chemia. 2017;62(1):129-142.
14. Khalaj Z, Ghoranneviss M, Nasirilaheghi S, Ghorannevis Z, Hatakeyama R. Growth of Nano Crystalline Diamond on Silicon Substrate Using Different Etching Gases by HFCVD. Chinese Journal of Chemical Physics. 2010;23(6):689-692.
15. Fan S, Lin S, Su Y, Shi Q, Dai M, Xiao S, et al. Various HFCVD diamond coatings synergistically tuned using CH_4 gas flow and working pressure and key merit evaluation of their coated tools. Int J Refract Met Hard Mater. 2023;114:106234.
16. Reshi BA, Kumar S, Misra A, Varma R. Multivariable study on growth of diamond on diamond substrates by microwave plasma chemical vapour deposition. Materials Research Express. 2019;6(4):046407.
17. Banks PS, Dinh L, Stuart BC, Feit MD, Komashko AM, Rubenchik AM, et al. Short-pulse laser deposition of diamond-like carbon thin films. Applied Physics A: Materials Science & Processing. 1999;69(7):S347-S353.
18. Han YX, Ling H, Sun J, Zhao M, Gebre T, Lu YF. Enhanced diamond nucleation on copper substrates by graphite seeding and CO2 laser irradiation. Appl Surf Sci. 2008;254(7):2054-2058.
19. Sazaki G, Yoshida E, Komatsu H, Nakada T, Miyashita S, Watanabe K. Effects of a magnetic field on the nucleation and growth of protein crystals. J Cryst Growth. 1997;173(1-2):231-234.
20. Ma Y, Watanabe K, Awaji S, Masumoto H, Motokawa M. Effect of magnetic field on growth of $YBa_2Cu_3O_7$ films on MgO substrates by metalorganic chemical vapor deposition. Physica C: Superconductivity. 2001;353(3-4):283-288.
21. Awaji S, Ma Y, Chen WP, Maeda H, Watanabe K, Motokawa M. Magnetic field effects on synthesis process of high-Tc superconductors. Current Applied Physics. 2003;3(5):391-395.
22. Awaji S, Watanabe K, Motokawa M, Kuramochi A, Fukase T, Kimura K. Melt textured process for YBCO in high magnetic fields. IEEE Transactions on Applied Superconductivity. 1999;9(2):2014-2017.
23. Asgary S, Vaghri E, Ramezani AH. Investigation of Vacuum Annealing Temperature Effects on the Microstructure Properties of DC-PECVD Grown Diamond Nanoparticles. Journal of Inorganic and Organometallic Polymers and Materials. 2021;31(4):1704-1712.
24. Ramos SLLM, Pimenta MA, Champi A. Multiple-excitation study of the double-resonance Raman bands in rhombohedral graphite. Carbon. 2021;179:683-691.
25. Vaghri E, Khalaj Z, Dorranian D. Investigating the Effects of Different Liquid Environments on the Characteristics of Multilayer Graphene and Graphene Oxide Nanosheets Synthesized by Green Laser Ablation Method. Diamond Relat Mater. 2020;103:107697.
26. Vaghri E, Dorranian D, Ghoranneviss M. Effects of CTAB concentration on the quality of graphene oxide nanosheets produced by green laser ablation. Materials Chemistry and Physics. 2018;203:235-242.
27. Solati E, Vaghri E, Dorranian D. Effects of wavelength and fluence on the graphene nanosheets produced by pulsed laser ablation. Appl Phys A. 2018;124(11).
28. Vaghri E, Khalaj Z, Ghoranneviss M, Borghei M. Characterization of Diamond: Like Carbon Films Synthesized by DC-Plasma Enhanced Chemical Vapor Deposition. J Fusion Energy. 2011;30(5):447-452.
29. Narayan R. Characterization of plasma enhanced chemical vapor deposition diamond-like carbon coatings on fused silica with and without argon or oxygen plasma treatment. American Chemical Society (ACS); 2020.

30. Salar Elahi A, Agah KM, Ghoranneviss M. RETRACTED: A new perspective on structural and morphological properties of carbon nanotubes synthesized by Plasma Enhanced Chemical Vapor Deposition technique. Results in Physics. 2017;7:757-761.
31. Dorner-Reisel A, Ritter U, Moje J, Freiberger E, Scharff P. Effect of fullerene C60 thermal and tribomechanical loading on Raman signals. Diamond Relat Mater. 2022;126:109036.
32. Chu PK, Li L. Characterization of amorphous and nanocrystalline carbon films. Materials Chemistry and Physics. 2006;96(2-3):253-277.
33. Gu SS, Hu XJ. Enhanced p-type conduction of B-doped nanocrystalline diamond films by high temperature annealing. J Appl Phys. 2013;114(2).
34. Sharma N, Kumar N, Sundaravel B, Panda K, David W, Kamarrudin M, et al. Effect of CH_4/H_2 plasma ratio on ultra-low friction of nano-crystalline diamond coating deposited by MPECVD technique. Tribology International. 2011;44(9):980-986.
35. Sun Z, Shi JR, Tay BK, Lau SP. UV Raman characteristics of nanocrystalline diamond films with different grain size. Diamond Relat Mater. 2000;9(12):1979-1983.
36. Xiao X, Wang J, Liu C, Carlisle JA, Mech B, Greenberg R, et al. In vitro and in vivo evaluation of ultrananocrystalline diamond for coating of implantable retinal microchips. Journal of Biomedical Materials Research Part B: Applied Biomaterials. 2005;77B(2):273-281.
37. Ray NR, Datta J, Biswas HS, Datta S. Signature of Misoriented Bilayer Graphenelike and Graphanelike Structure in the Hydrogenated Diamond-Like Carbon Film. IEEE Transactions on Plasma Science. 2012;40(7):1789-1793.
38. Fedoseeva YV, Gorodetskiy DV, Baskakova KI, Asanov IP, Bulusheva LG, Makarova AA, et al. Structure of Diamond Films Grown Using High-Speed Flow of a Thermally Activated CH_4-H_2 Gas Mixture. Materials (Basel, Switzerland). 2020;13(1):219.
39. Mortazavi SZ, Parvin P, Reyhani A, Mirershadi S, Sadighi-Bonabi R. Generation of various carbon nanostructures in water using IR/UV laser ablation. J Phys D: Appl Phys. 2013;46(16):165303.
40. Bunaciu AA, Udriştioiu Eg, Aboul-Enein HY. X-Ray Diffraction: Instrumentation and Applications. Crit Rev Anal Chem. 2015;45(4):289-299.
41. Ameh ES. A review of basic crystallography and x-ray diffraction applications. The International Journal of Advanced Manufacturing Technology. 2019;105(7-8):3289-3302.
42. Das R, Hamid S, Ali M, Ramakrishna S, Yongzhi W. Carbon Nanotubes Characterization by X-ray Powder Diffraction – A Review. Current Nanoscience. 2014;11(1):23-35.
43. Millán-Barba J, Taylor A, Bakkali H, Alcantara R, Lloret F, de Villoria RG, et al. Low temperature growth of nanocrystalline diamond: Insight thermal property. Diamond Relat Mater. 2023;137:110070.
44. Mandal S, Arts K, Morgan DJ, Chen Z, Williams OA. Zeta potential and nanodiamond self assembly assisted diamond growth on lithium niobate and lithium tantalate single crystal. Carbon. 2023;212:118160.
45. Takamori Y, Nagai M, Tabakoya T, Nakamura Y, Yamasaki S, Nebel CE, et al. Insight into temperature impact of Ta filaments on high-growth-rate diamond (100) films by hot-filament chemical vapor deposition. Diamond Relat Mater. 2021;118:108515.
46. Millán-Barba J, Bakkali H, Lloret F, Gutiérrez M, Guzmán de Villoria R, Domínguez M, et al. Boron-doped diamond growth on carbon fibre: Enhancing the electrical conductivity. Appl Surf Sci. 2023;615:156382.
47. Nakano Y, Zhang X, Kobayashi K, Matsumoto T, Inokuma T, Yamasaki S, et al. Impact of nitrogen doping on homoepitaxial diamond (111) growth. Diamond Relat Mater. 2022;125:108997.
48. Kobayashi K, Zhang X, Makino T, Matsumoto T, Inokuma T, Yamasaki S, et al. Selectively buried growth of heavily B doped diamond layers with step-free surfaces in N doped diamond (1 1 1) by homoepitaxial lateral growth. Appl Surf Sci. 2022;593:153340.
49. Lobaev MA, Gorbachev AM, Bogdanov SA, Vikharev AL, Radishev DB, Isaev VA, et al. Influence of CVD diamond growth conditions on nitrogen incorporation. Diamond Relat Mater. 2017;72:1-6.
50. Sartori AF, Overes BHL, Fanzio P, Tsigkourakos M, Sasso L, Buijnsters JG. Template-assisted bottom-up growth of nanocrystalline diamond micropillar arrays. Diamond Relat Mater. 2019;95:20-27.
51. Yang B, Shen Q, Gan Z, Liu S. Improving the edge quality of single-crystal diamond growth by a substrate holder – An analysis. Comptes Rendus Physique. 2019;20(6):583-592.
52. Moore E, Jarrell J, Cao L. Heteroepitaxial diamond growth on 4H-SiC using microwave plasma chemical vapor deposition. Heliyon. 2017;3(9):e00404-e00404.